Compositional layering within the Large Low Shear-wave Velocity Provinces in the lower mantle

*Maxim Ballmer[1,2], Lina Schumacher[3], Vedran Lekic[4], Christine Thomas[3], Garrett Ito[5]

1. Institut für Geophysik, Departement für Erdwissenschaften, ETH Zürich, 8092 Zürich, Switzerland, 2. Earth-Life Science Institute, Tokyo Institute of Technology, Meguro, Tokyo 152-8551, Japan, 3. Institut für Geophysik, Westfä lische Wilhelms Universität Münster, 48149 Münster, Germany, 4. Department of Geology, University of Maryland, College Park, MD 20742, USA, 5. School of Ocean and Earth Sciences and Technology, University of Hawai‘i at Manoa, Honolulu, HI 96822, USA

The large low shear-wave velocity provinces (LLSVP) are thermochemical anomalies in the deep Earth’s mantle, thousands of km wide and ~1,800 km high. This study explores the hypothesis that the LLSVPs are compositionally subdivided into two domains: a primordial bottom domain near the core-mantle boundary and a basaltic shallow domain extending from 1,100~2,300 km depth. This hypothesis reconciles published observations in that it predicts that the two domains have different physical properties (bulk-sound vs. shear-wave speed vs. density anomalies), the transition in seismic velocities separating them is abrupt, and both domains remain seismically distinct from the ambient mantle. We here report underside reflections from the top of the LLSVP shallow domain, supporting a compositional origin. By exploring a suite of two-dimensional geodynamic models, we constrain the conditions under which well-separated “double-layered” piles with realistic geometry can persist for billions of years. Results show that long-term separation requires density differences of ~100 kg/m^3 between LLSVP materials, providing a constraint for origin and composition. The models further predict short-lived “secondary” plumelets to rise from LLSVP roofs and to entrain basaltic material that has evolved in the lower mantle. Long-lived, vigorous “primary” plumes instead rise from LLSVP margins and entrain a mix of materials, including small fractions of primordial material. These predictions are consistent with the locations of hotspots relative to LLSVPs, and address the geochemical and geochronological record of (oceanic) hotspot volcanism. The study of large-scale heterogeneity within LLSVPs has important implications for our understanding of the evolution and composition of the mantle.

Keywords: Mantle Convection, Primordial Reservoir

深海洋底とプレートテクトニクスの起源，慣性能率偏芯モーメント駆動力の証明

環太平洋孤状列島背弧海盆の起源，プレート相互の潜り込みメカニズム，移動方向の急変の理由，全てを統一的に説明する「マルチインパクト仮説」のアブダクションによる検証　---- 一度だけの地球進化・実証歴史による -

Origin of Seafloor, Platetectonics, Pacific arc basin, Proof of eccentric Moment Force, Mechanism of Plate rapid change of direction,

Verification by Abduction of "Multi Impact Hypothesis" explaining everything uniformly.

*種子 彰[1]
*Akira Taneko[1]

1. SEED SCIENCE Lab.
1. SEED SCIENCE Lab.

地球惑星テクトニクス　*大陸移動説,海洋底拡大更新説,プレートテクトニクスからプルーム仮説まで駆動力は熱対流仮説であった.*

衝突による地殻マントル欠損とアイソスタシー隆起偏芯による慣性能率アンバランスによる慣性モーメント最少化の偶力仮説を**プレート新駆動力**として提案します.

A Wegenrが大陸の南北アメリカのとアフリカの沿岸プロフィールが一致することから，**大陸移動仮説**を提唱して，古生物学や地質の連続性を根拠に証明しようとした.

今では**海洋底拡大仮説**や**マントル熱対流仮説**や大西洋中央海嶺の発見やトランスフォーム断層の発見や地磁気の反転と海底テープレコーダー仮説など実証的な観測で**プレートテクトニクス**がほぼ定説となっている．しかし，*ウェゲナーが示せなかった**大陸移動の駆動力**はプレートテクトニクスでも**まだ謎のまま**である.*

ウェゲナーが指摘していた，70%を占める深海洋底(-5km)の形成起源やプレート境界の起源，プレートテクトニクスの起源を探究する努力が忘れられていた.

弧状列島と海盆の起源も謎のままである．この全てを統一的に解明できる新パラダイムが望まれていた.

それはアブダクションによるマルチインパクト仮説であり，地球物理学と太陽系惑星学から"地球と月のミッシングリンクの解明"で述べられた.

それによると，このプレートテクトニクスの起源の他に，月の形成や深海洋底の起源，コアの偏芯や木星大赤斑の起源や水星や冥王星の起源，更には小惑星帯の起源や分化した隕石の起源も統一的に解明できる新パラダイムの提案である.

更に,月の軌道エネルギー(衝突エネルギーから理論的に計算済)とマントル物質だけの月や月が同じ側を向けている偏芯密度差の理由も示せた.

アブダクションは，ある仮説による結論が複数の現状を説明できれば出来るほどその仮説の正しさが保証されるという考え方である.

発想の大転換であり創造的推論Abduction と呼ばれている.
物理的に意味がある仮説を用いると，アイデアが正しければ，画期的な進歩が得られる.

"マルチインパクト仮説" : 太陽系の誕生から約40億年前まで経過してCERRAが木星摂動により軌道変形し木星と太陽の張力で断裂した時，CERRAと地球は分化凝固していた.
本仮説では複数マントル破片がほぼ同じ軌道を巡り間欠的に衝突することが，度重なる生物種大絶滅の原因であり,マントルを剥ぎアイソスタシーにより5km 深さの深海洋底の起源となった.
アイソスタシーにより衝突マントル欠損部にダーウィンの隆起(凸プレート)が起きたとき，周囲の地殻が剥離したプレートが凹型にへこんで，その境界亀裂が弧状列島を形成した環太平洋孤状列島凹背弧海盆の起源.
太平洋を中心とした弧状列島やテーチス海の形成時のジャワ島等，弧状列島の外側に連なる海溝弧は凸プレートが弧状列島凹海盆の下に潜り込みを示してる(=プレート相互の潜り込みメカニズム).
プレート境界は複数のマントル断裂片が地球へ衝突した時の亀裂に起因している.

慣性能率偏芯モーメント駆動力の証明
本仮説では,地球が自転している為，衝突により欠けたマントルがアイソスタシーで凸になった時，慣性モーメントが不均一(アンバランス)になった地球では,慣性モーメントを最小にする駆動力が発生する.
移動方向の急変の理由と自転軸傾斜のメカニズム
マントル片衝突時の衝撃破は地球の反対側に内側からの噴出圧力として働く.
ダイヤモンド鉱山の形成メカニズムはキンバーライト・パイプの形成で示される.
Drake Passageへの衝突がロシアミルーヌィのダイヤモンド鉱山の成因である.
高緯度への衝突の偶力により自転軸が公転面より23.5˚の傾斜が形成された.
ハワイ諸島と千島海山列のプレート移動痕跡と平行な三列の屈曲した軌跡がある.
それはプレート移動方向の結果であり,自転軸の急変が原因である.

-- 一度だけの地球進化・実証歴史による --
一つの仮説だけで，全ての謎を統一した進化として説明できる事は，「マルチインパクト仮説」のアブダクションによる検証となる.
これにより定性的な解明から 更に詳細に定量的なシミュレーションが可能となる事が期待できる.

キーワード：深海洋底の起源 ≒4700,地球表面積の70%を占める、月と地球プレートテクトニクスの起源、慣性能率偏芯モーメント駆動力の証明、環太平洋孤状列島背弧海盆の起源，プレート相互の潜り込みメカニズム、プレート移動方向急変メカニズム　理由、アブダクションによる検証　-- 一度だけの地球進化・実証歴史による --
Keywords: Origin of Ocean floor, Origin of the "Moon formation and the Earth's plate tectonics", Proof of inertial efficiency eccentric moment driving force, Origin of the Pacific Rim Arc Isolated Archipelago Back Arc Basin, Mechanism of Slipping Inside Plates, Plate movement direction rapid change mechanism reason, Verification by abduction - by one-time evolution of the earth and empirical history -

Origin of the Earth,Plate-tectonics,Ocean-floor, by Abduction in Multi-Impact Hypothesis CERRA

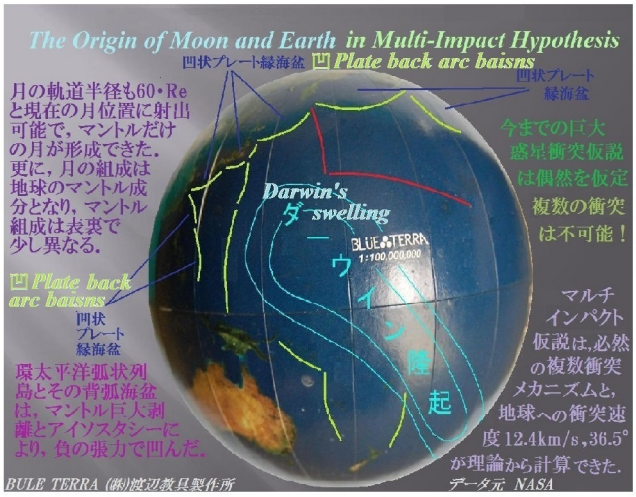

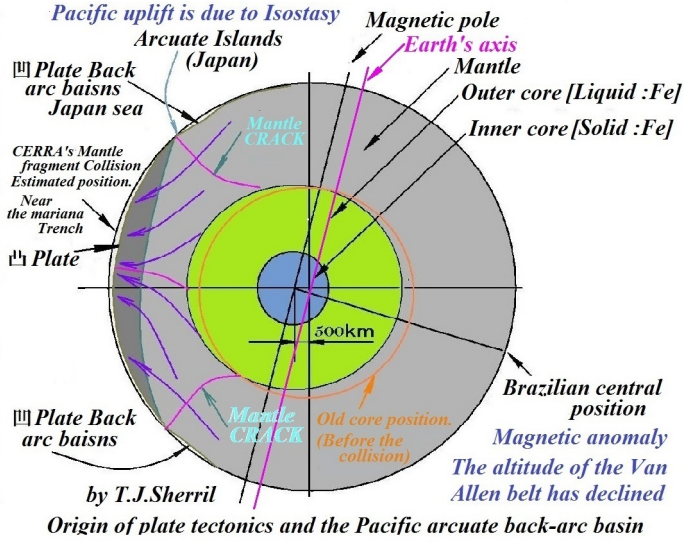

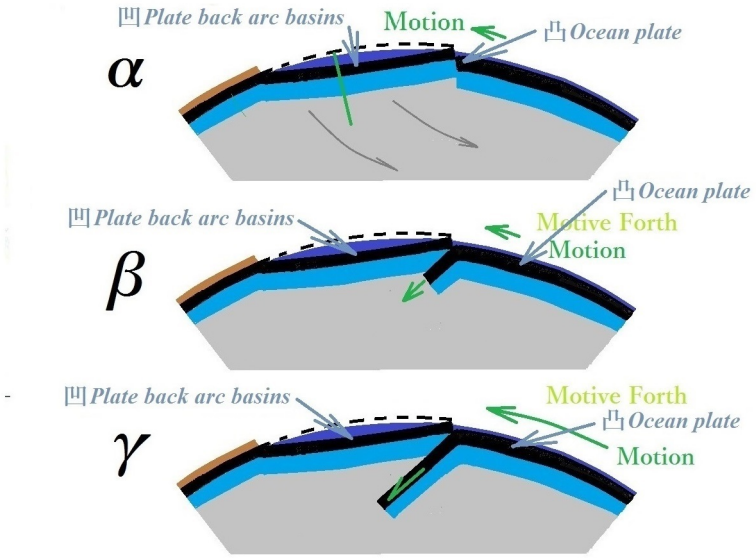

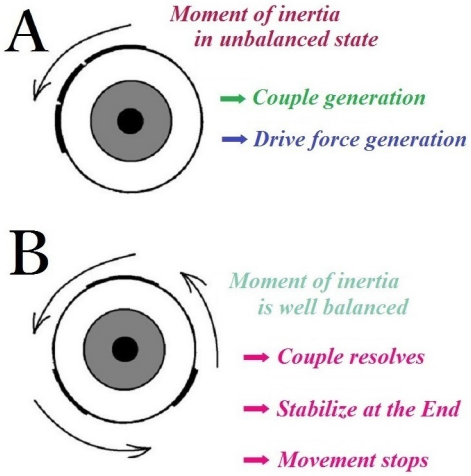

Phase Transformation Mechanism Responsible for Deep-focus Earthquakes by The Multi-Phase-Field Methods

*澤 燦道[1]、木戸 正紀[1]、白石 令[1]、武藤 潤[1]、長濱 裕幸[1]
*Sando Sawa[1], Masanori Kido[1], Rei Shiraishi[1], Jun Muto[1], Hiroyuki Nagahama[1]

1. 東北大学理学研究科地学専攻
1. Department of Earth Science, Tohoku University

One of the possible mechanisms for deep-focus earthquakes is the faulting associated with phase transformation from olivine to spinel under high pressure. Burnley et al. (1991) conducted deformation experiments of Mg_2GeO_4 under conditions at confining pressures of 1~2 GPa, temperature of 900~1500 K and strain rates of 2×10^{-5} ~ 2×10^{-3} s^{-1}. The spinel is observed like microscopic lenses in place of microcracks. They form perpendicular to the maximum compressive direction, which is called “anticracks.” They connect with each other, eventually, cause the faulting. Spinel anticracks can be formed by intracrystalline nucleation and nucleation at grain boundaries. As the mechanism, it has been advocated that they form by nucleation whose crystal orientation is random, martensitic transformation or along the dislocation. However, we don’t know which is a dominant mechanism forming spinel anticrack. So, to reveal how spinel anticracks are formed, we have studied the transformation mechanics by the Multi-Phase-Field (MPF) method. The MPF method is a phenomenological model based on continuum mechanics and has widely used in material sciences. We can reveal temporal change of material morphology by MPF method, that is, easily follow crystal interfaces with probability. We developed the numerical model taking into account of both intracrystalline nucleation and nucleation at grain boundaries. Furthermore, to constrain physical conditions of the numerical model, we also conducted experiments by a Griggs type piston-cylinder apparatus using solid NaCl as a confining medium based on Burnley et al. (1991) to observe microstructure of a deformed sample. We compressed Mg_2GeO_4 as an analogue material under conditions at confining pressure of 1.2 GPa, temperature of 1200 K and strain rate of 2.0×10^{-4} $s^{-1}$where Burnley et al. (1991) reported faulting by anticrack mechanism. As a result of the experiment, the sample was ductile deformed. According to the microstructural observation on the deformed sample, there are many bands composed of very-fine grained materials. The particle size is very small and there are small faults in the vicinity, so we think that superplastic deformation in these fine-grained portions might cause faulting, as proposed by Burnley et al. (1991). Also, compared to hydrostatic experiment in which fine grain materials were observed but phase transformation didn’t occur, we inferred that phase transformation is difficult to occur without differential stress. Therefore, we modified the conditions of numerical model to consider superplastic deformation and particle size, finally, built up new numerical model.

キーワード：深発地震、フェーズフィールド法、Griggs式固体圧変形試験機
Keywords: Deep-focus earthquakes, Phase Field, Griggs type piston-cylinder apparatus

Stability of anhydrous phase B, $Mg_{14}Si_5O_{24}$, at the mantle transition zone conditions

*Liang Yuan[1,2], Eiji Ohtani[1], Akio Suzuki[1], Zhenmin Jin[2]

1. Department of Earth and Planetary Materials Science, Tohoku University, 2. School of Earth Sciences, China University of Geosciences (Wuhan)

Stability of anhydrous phase B, $Mg_{14}Si_5O_{24}$, has been determined in the pressure range of 14-21 GPa and in the temperature range of 1100-1700˚C with both normal and reverse experiments at high pressures and high temperatures. Our results imply that anhydrous phase B is stable at the *P-T* conditions corresponding to the shallow depth of the mantle transition zone and it decomposes into periclase and wadsleyite at greater depth. The decomposition boundary of anhydrous phase B into wadsleyite and periclase has a positive phase transition slope and can be expressed by the following equation, P(GPa)= 7.5 + 6.6 x 10^{-3}T(˚C). Configuration disorder might account for an increase of entropy for anhydrous phase B at high-temperature conditions. It is suggested that MgO-rich conditions can be available in the deep mantle during hydrous melting of peridotite and the reduction of subduction carbonates by the metal-saturated mantle at depth > 250 km. Anhydrous phase B might become an important phase in the area where SiO_2 activity is low. We propose that the paragenesis of directly touched ferropericlase-olivine inclusions in natural diamonds might be the retrogression products of anhydrous phase B via the decomposition reaction Anh-B = Olivine + Periclase during the transportation of host diamonds from the deep to the surface. Our experimental results put a constraint on the origin of such diamonds at a depth less than 500 km. On the cooling of the magma ocean during the early history of the Earth, a distinctive layer that was concentrated with hydrogen and other elements such as Fe, Ca, Mn substituting Mg might exist with the crystallization and accumulation of anhydrous phase B at depth equivalent to the upper part of the mantle transition zone.

Keywords: Anhydrous phase B, phase relations, Clapeyron slope, diamond inclusions, Raman spectra

2次元円環状モデルを用いたスラブの挙動・形態に関する数値シミュレーション

Numerical simulations on the formation and behaviors of slabs in 2-D spherical annulus

*土田 真愛[1]、亀山 真典[1]
*Mana Tsuchida[1], Masanori Kameyama[1]

1. 国立大学法人愛媛大学地球深部ダイナミクス研究センター
1. Geodynamics Research Center, Ehime University

近年の地震波トモグラフィー研究により、マントル中に沈み込んだプレート(スラブ) は沈み込み帯ごとに異なる描像を示すことが明らかにされている。その例として、660 km不連続面で水平に横たわり停滞するもの (いわゆる「停滞スラブ」) や660 km不連続面で停滞せずにすぐ下部マントルに到達するもの (いわゆる「貫入スラブ」) 、などが挙げられる。このようなスラブの挙動・形態の違いが生じる原因を探るため、マントル中に沈み込むプレートの数値シミュレーション研究がこれまでにも多く行われてきたが、そのほとんどは2次元の箱型形状モデルに基づくものに限られていた。そこで本研究では、地球の曲率の効果を模した2次元の円環状モデルを新たに開発し、これを用いてプレート沈み込みの数値シミュレーションを行う。これにより、地震波トモグラフィー研究によって観測されているような様々なスラブの挙動・形態の再現とそれらの発現する条件の解明を目的とする。また、マントル中のスラブの形態からそこでのプレート速度や660 km不連続面の性質の制約を試みる。

本研究では2次元円環の8分の1 (45度分) に相当するモデル領域内において、冷たいスラブの沈み込みと海溝後退の動きによって駆動されるマントル物質 (拡張ブシネスク近似流体) の熱対流を考える。マントル物質の粘性は温度・圧力の両方に依存すると仮定した。深さ410 kmと660 kmでのマントル物質の相転移の効果を考慮した。海洋プレートの沈み込みは、最大深さ400 kmまで「海溝」から右斜め下方に延びる「流路」に沿って低温の流体を一定速度 (海洋プレート速度) で流し込むことによってモデル化している。ここでは、海溝後退速度、海洋プレート速度、上部-下部マントル間の粘性ジャンプ、660 km不連続面におけるクラペイロン勾配4つのパラメータを系統的に変化させて数値シミュレーションを行い、各条件下でのスラブの挙動・形態を調べた。

シミュレーションを行った結果、海溝後退速度、海洋プレート速度、粘性ジャンプ、660 km不連続面におけるクラペイロン勾配の4つのパラメータの組み合わせによって異なるスラブの挙動・形態が発現し、それらによって地震波トモグラフィーで観測されるスラブの多様さを十分網羅しうることが分かった。またシミュレーションで発現するスラブの挙動・形態は、(1) 下部マントルに即座に「貫入」、(2)不連続面で「蓄積」、(3) 不連続面上に「浮揚」、(4) 不連続面で水平に横たわるように「停滞」、(5)　「停滞」したのちに下部マントルへ「崩落」、という5つのタイプに分類することができた。加えて、本研究のシミュレーションと地震波トモグラフィーで得られているスラブの形態を比較することによって、沈み込み帯における各パラメータ値の制約を試みた。プレート収束速度と沈み込みの継続時間の双方が十分制約されている複数の沈み込み帯について比較を行った結果、沈み込んだスラブの形態から海溝後退速度を有意に制約できることが分かった。このことはプレートとプレートの相対速度 (プレート収束速度) という観測量からプレートの絶対速度 (海溝後退速度や海洋プレート速度) を導き出す上で、沈み込んだスラブの形態が重要な制約条件になり得ることを意味している。またこのような比較は、クラペイロン勾配や粘性ジャンプといった660 km不連続面の性質に対する数値流体力学的な制約を与え得るかもしれない。

キーワード：スラブ沈み込み、スタグナントスラブ、マントル対流、数値シミュレーション
Keywords: subducted slab, stagnant slab, mantle convection, numerical simulation

天然に見られる様々な結晶軸配向パターンを再現した高緻密極細粒オリビン多結晶試料の創製

Fabrication of highly-dense and fine-grained olivine aggregates with various crystallographic preferred orientation patterns in natural peridotite rocks

*小泉 早苗[1]、鈴木 達[2]、目 義雄[2]、谷部 功将[1]、平賀 岳彦[1]
*Sanae Koizumi[1], Thoru S Suzuki[2], Yoshio Sakka[2], Kosuke Yabe[1], Takehiko Hiraga[1]

1. 東京大学地震研究所、2. 物質・材料研究機構
1. Earthquake Research Institute,The University of Tokyo, 2. National Institute for Materials Science

Olivine is the most abundant mineral in the Earth’s upper mantle and it is considered to orient crystallographically in response to the mantle flow. Six types of fabrics have been identified in mantle peridotite: A, B, C, D, E and AG type. Physical properties of olivine such as elasticity, plasticity, thermal conductivity, thermal expansion and electron conductivity are known to be anisotropic so that geophysical observations showing directional dependence in the mantle are often attributed to the result of crystallographic preferred orientation (CPO) of the mineral. However, most of our current understanding of the effects of CPO on physical properties of bulk rocks is essentially based on the properties of single crystals.
To measure CPO effect on the bulk rock properties directly by room experiments, it is required to prepare polycrystalline materials with ideally controlled CPO
Olivine particles synthesized from source oxide powders and natural mineral particles prepared from milling natural olivine crystals were used in this study. To fabricate olivine aggregates with CPO, an external strong magnetic field (12 T) was applied to the olivine fine particles which were dispersed in the solvent. The alignment of certain crystallographic axes of the particles with respect to the magnetic direction was anticipated due to magnetic anisotropy of olivine. The dispersed particles were gradually consolidated on a porous alumina mold, which was covered with a solid-liquid separation filter, during drainage of the solvent. The consolidated aggregate was then isostatically pressed and vacuum sintered.
Uni-axially aligned *c*-axes and *b*-axes olivine aggregates that correspond BC-type and AC-type peridotite were obtained from the aggregates aligned under static and rotated magnetic field, respectively.
Tri-axially aligned olivine aggregates corresponding to A-, B-, C- and E-type peridotite were obtained from a modulated rotation magnetic field.

キーワード：結晶格子選択配向、オリビン、鉱物多結晶体
Keywords: crystallographic preferred orientation, olivine, mineral aggregate

High-resolution 3-D S-wave structure beneath North America using phase and amplitude of surface waves

浜田 広太[1]、*吉澤 和範[1,2]
Kouta Hamada[1], *Kazunori Yoshizawa[1,2]

1. 北海道大学大学院理学院、2. 北海道大学大学院理学研究院
1. Graduate School of Science, Hokkaido University, 2. Faculty of Science, Hokkaido University

Majority of surface wave tomography have employed the phase information, which reflects the average phase speed perturbation along a propagation path. To the contrary, the use of amplitude anomalies of surface waves has been limited in tomographic studies, due to a variety of uncertain factors such as source mechanism, local amplification at receiver, elastic focusing/defocusing and anelastic attenuation. In the interstation analysis, the source term can be canceled out, so that we can focus on the effects of the elastic focusing/defocusing as well as the receiver amplification factors, with an appropriate correction for anelastic attenuation. In the framework of ray theory, the amplitude anomalies affected by the focusing/defocusing reflect the second derivatives of phase speed across the ray path, and thus the amplitude data are more sensitive to shorter-wavelength structure than the conventional phase data.

In this study, we employ a fully non-linear waveform fitting technique to measure interstation phase speeds and amplitude ratios simultaneously, based on a global optimization method. This technique is applied to observed seismograms of the high-density transportable array deployed in the United States (USArray) in the past decade, and a large-number of interstation phase speed and amplitude ratio data are collected. The typical interstation distances for measured dispersion data are less than 1000 km, which is much shorter than the average path length used in conventional single-station analysis and can be of help in improving the lateral resolution of the regional tomography models.

The measured interstation phase and amplitude data are inverted simultaneously for phase speed maps as well as local amplification factor at each receiver location. The phase speed maps derived from both phase and amplitude measurements exhibit better recovery of the strength of velocity perturbations, particularly for the smaller-scale heterogeneities. The spatial distributions of local amplification factors in the longer period are correlated well with the velocity structure in the upper mantle, indicating that the effects of local amplification can be isolated well from those of focusing in our joint inversion of phase and amplitude data.

Isotropic and anisotropic 3-D S wave speed models of North American continent are then obtained from the phase speed maps. Our isotropic 3-D S wave models from phase and amplitude data for Rayleigh waves emphasize local-scale tectonic features associated with conspicuous lateral velocity gradients; e.g., fast anomaly in the Colorado Plateau surrounded by slow anomalies, and slow anomaly in the New Madrid Seismic Zone encompassed by faster regions. Such local tectonic features with the size of about 200 km can hardly be identified in the conventional surface wave tomography, and thus the interstation amplitude ratio data can be of great help in improving the lateral resolution of velocity models in the upper mantle. Radial anisotropy models derived from the phase speed maps of Rayleigh and Love waves using only phase data, are also constructed. The results show faster SH wave speed anomaly than SV in the tectonically active regions in the western and central U.S., while the model exhibits faster SV wave speed anomaly than SH in the eastern region below 75 km depth.

キーワード：上部マントル、表面波振幅、北米大陸
Keywords: upper mantle, surface wave amplitude, North American Continent

DAC-GHz実験におけるS波バッファロッドの開発
Dvelopment of S wave buffer rod for DAC-GHz experiments.

*米田 明[1]
*Akira Yoneda[1]

1. 岡山大学惑星物質研究所
1. Institute for Study of the Earth's Interior, Okayama University

I have been develping GHz ultrasonic technique for diamond anvil cell (DAC) in a recent a few years. Last year, I reported the development of P wave GHz buffer rod. Then, I conducted development of GHz S wave buffer rod as well. Simultaneopusly, I have examined how to get a good signal through P wave buffer rod. The solution is combination wiping by aceton, alcohole, and ammonia water. I have started the measurement for the specimen squeezed in DAC. In the poster, I will show those effort.

キーワード：GHz音速法、ダイヤモンドアンビルセル、S波、マントル、弾性、高圧
Keywords: GHz ultrasonics, diamond anvil cell, Shera wave, mantle, elasticity, high pressure

P and SH wave upper mantle velocity structure beneath South China

*yi sui[1], rui qing zhang[1], qing ju wu[1]

1. Institute of Geophysics China Earthquake Administration

There is widespread intracontinental orogen and magmatic province in Mesozoic South China. Study of upper mantle velocity can bring light on the distribution and movement of material in deep earth of this region. Triplication waveform of P and SH from 5 to 30 degree recorded by CDSN(Chinese Digital Seismic Network) are used to obtain P and SH wave upper mantle velocity structure by comparing with synthetic waveform. There is low velocity layer above 410 in both P and S waveform, and 410km discontinuity is broadened. Low P and low S velocity and high Vp/Vs may be result of partial melting related to plate subduction.

Keywords: triplciation, upper mantle , partial melting

低粘性層を含む内部構造を持つ固体地球の潮汐散逸
Tidal Dissipation of the Solid Earth with an Internal Structure Including a Low-Viscosity Layer

*原田 雄司[1]、松本 晃治[2]
*Yuji Harada[1], Koji Matsumoto[2]

1. 澳門科技大學太空科學研究所月球與行星科學實驗室、2. 自然科学研究機構国立天文台RISE月惑星探査検討室
1. Lunar and Planetary Science Laboratory, Space Science Institute, Macau University of Science and Technology, 2. RISE Project Office, National Astronomical Observatory of Japan, National Institutes of Natural Sciences

固体地球における潮汐散逸は重要な地球物理学的現象の一つである．固体天体の潮汐散逸は内部構造，特に粘性構造に依存するから，その制約条件と成り得る．粘性構造を制約する事が出来れば，それはマントルダイナミクスを知る為の一つの有益な手掛かりを与えるかも知れない．

固体地球の潮汐応答，特に理論的なラブ数の潮汐周期と粘性構造に対する依存性に関しては既に幾つかの先行研究で調べられている．その結果，測地学的観測から得られたラブ数の周波数依存性を上手く解釈する為にはマントルの内部，特に底部における低粘性層の存在が重要であると考えられている．

その一方，上述の研究と類似の考え方に基づいて我々筆者達は，この様な低粘性層が月のマントルにも存在すると仮定して潮汐クオリティ係数の周波数と内部構造に対する依存性を調べた．結果として地球と同様，もしマントルの底に低粘性層が存在すれば測月観測から得られたクオリティ係数の周波数依存性が説明可能である事を示した．そして更には，その層の粘弾性に対応する特徴的時間スケールは主要な潮汐周期と非常に近い事を見出した．即ち層内で効率的な潮汐発熱が起こる様な粘性率が自己調節的に決まる可能性も示した．

この月潮汐における示唆を踏まえて視点を地球潮汐に戻すと，こうした卓越する潮汐の周期と調和する粘性率が地球の低粘性層でも与えられるのかどうか，は知られていない．過去の研究で明示されていたのは主に複素ラブ数の周波数依存性である．確かに過去の解析においても層の粘性の不確定性は系統的に考慮されていた．但し，その複素ラブ数から導かれるクオリティ係数の粘性構造依存性までは明示されていなかった．その点の調査は地球物理学と比較惑星学の双方の観点で有意義である．

そこで本研究では固体地球の潮汐散逸，特にクオリティ係数に及ぼすマントル最下部の低粘性領域の効果を定量的に見積もる為，幾つかの実際の潮汐周期を想定して粘弾性潮汐変形の計算を行なった．ここで密度と弾性率の鉛直構造に関しては地震波の観測に基づく典型的な参照構造を与えた．又，粘性構造に関しては大まかな構造依存性を把握する為，層構造を単純化して上から下へリソスフェア，アセノスフェア，メソスフェア，及び低粘性層の四層だけ設定した．その中で低粘性層の粘性のみ調整して残りの三層の粘性は均一かつ一定とした．クオリティ係数を求める際の複素ラブ数の計算において応力と歪の関係はマクスウェル物体のレオロジー則に従った．そしてクオリティ係数の理論値を観測値と比較する事によって，この層の粘性率を見積もった．

本計算の結果，地球の潮汐変形においても月と同じく低粘性層の緩和時間が潮汐周期に近い事が分かった．ここで低粘性層の影響を加味すれば測地学的観測量と調和的な計算結果が得られるのは先行研究と概ね同様である．今回の研究で更に明らかとなった事は，地球潮汐で特に卓越する半日周潮と日周潮の各周期で共にクオリティ係数を満足する粘性率のマクスウェル緩和時間は潮汐周期に近かった点である．言い換えれば地球の場合でも前述の月の低粘性層の場合と類似する示唆が得られたと言える．

本結果はマントルの底に低粘性層が維持される理由を考察する上で興味深い．何故なら上述の結果は，月の先行研究の中で指摘されたマントル最下部の効率的な潮汐エネルギー散逸は地球のマントル最下部でも励起されている事を意味するからである．即ち月の核マントル境界の直上における粘性の自己調節機構は地球でも有り得る事が予想される．この低粘性領域の緩和時間と潮汐周期の対応関係は，上記の計算の中で定義された内部構造の範囲内において潮汐発熱が最大に近い事を意味する．とは言え，地球深部では放射性壊変の発熱の影響が月よりも支配的であり，従って熱的状態も月深部とは大きく異なる．その点に関しては今後，更なる調査が必要であろう．

本結果はマントルの底に低粘性層が維持される理由を考察する上で興味深い．何故なら上述の結果は，月の先行研究の中で指摘されたマントル最下部の効率的な潮汐エネルギー散逸は地球のマントル最下部でも励起されている事を意味するからである．即ち我々自身が月の潮汐散逸の研究で指摘した核マントル境界付近における粘性の自己調節機構は地球にも存在すると予想される．この低粘性領域の緩和時間が潮汐周期に近いという事実は，上記の計算の中で定義された内部構造の範囲内において潮汐発熱がほぼ最大であるという事を意味する．但し地球深部では放射性壊変の発熱の影響が月よりも支配的であり，従って熱的状態も月深部とは大きく異なるであろう．その点に関しては今後，更なる調査が必要であろう．

謝辞：本研究は澳門特別行政區科學技術發展基金より科研資助039/2013/A2及び007/2016/A1の助成を受けて実施された．

キーワード：潮汐散逸、固体地球、内部構造、低粘性層
Keywords: Tidal Dissipation, Solid Earth, Internal Structure, Low-Viscosity Layer

Upper mantle structure beneath the Ontong Java Plateau from measurements of body wave differential travel times

*小林 拓史[1]、末次 大輔[2]、大林 政行[2]、杉岡 裕子[1]
*Takumi Kobayashi[1], Daisuke Suetsugu[2], Masayuki Obayashi[2], Hiroko Sugioka[1]

1. 神戸大学、2. 国立研究開発法人海洋研究開発機構
1. KOBE University, 2. Japan Agency for Marine-Earth Science and Technology

The Ontong Java Plateau(OJP) is a single largest oceanic plateau in the world, and thought to emplaced at 120Ma. To reveal the origin of the OJP, we have to know the structure beneath the OJP. Richardson et al. (2000) showed that S-velocities are 2-3 % lower than global average above a depth of 300 km beneath the OJP.
In this study we investigated upper mantle structure beneath the OJP by using PP-P differential travel times for PP waves of which bounce points are located on the OJP and the surrounding region. We analyzed waveform data of events from 2012 to 2013 recorded by IRIS and F-net stations.
We follow a method of Obayashi et al. (2004) to obtain PP-P differential travel time residuals. First a band-pass filter from 5 to 10 second was applied to the waveform data. To calculate PP-P differential residuals, we synthesized PP waves from P waves by applying the Hilbert transform, attenuation operator, and multi reflection/conversion effect in the crust beneath the bounce points. To calculate the multi reflection/conversion effect, we used crust structure model CRUST1.0 (REFERENCE). We then calculated PP-P differential residuals with respect to differential times predicted from the iasp91 model (Kennett and Engdahl, 1991) by cross-correlation of the observed and synthetic PP waves. Distribution of the obtained PP-P differential residuals indicated that the residuals are consistently negative for PP waves of which bounce points are located on the OJP. The average PP-P residual for such PP-waves is -1.6 second, which suggests P-velocities faster than that of iasp91 beneath the OJP, while we cannot constrain a depth range of the fast anomalies from the present study. Assuming that the average residual is due to uniformly fast structure above a depth of 300 km, P-wave velocity beneath the OJP is 1.7% faster than that of the iasp91 model.

キーワード：オントンジャワ海台、実体波
Keywords: Ontong Java Plateau, body wave

Mechanical coupling between the plate and lowermost mantle controlled by the subducted lithosphere strength

*中久喜 伴益[1]、金子 岳郎[1]、山崎 大輔[2]
*Tomoeki Nakakuki[1], Takeo Kaneko[1], Daisuke Yamazaki[2]

1. 広島大学大学院理学研究科地球惑星システム学専攻、2. 岡山大学惑星物質研究所
1. Department of Earth and Planetary Systems Science, Graduate School of Science, Hiroshima University, 2. Institute for Planetary Materials, Okayama University

Hotspot volcanoes are regarded as an indication of mantle plumes that originate from the deep mantle. Relative migration between the hotspot tracks suggests much slower horizontal motion of the deep mantle layer than that of the surface plates. Viscosity increase in the lower mantle is often attributed to the cause of the slow motion in the deep mantle. Numerical modeling on subducted lithospheres integrated into a mantle convection system showed that the lithosphere penetrating into the lower mantle is not assimilated thermally to the surrounding mantle, so that the subducted lithosphere should work as a substance to transmit viscous stress from the deep mantle. This implies that motion of the deep mantle layer is strongly coupled with that of the surface plate.

We performed numerical simulation of an integrated lithosphere-mantle convection system in which the subducted lithosphere penetrates into the core-mantle boundary region. We investigated effects of yield strength and viscosity reduction due to the grain-size reduction or interconnection of ferro-periclase generated at the 660-km phase transition. The viscosity in the lower mantle was controlled as the value fit to the range inferred from geoid anomalies. In addition to them, depth-dependent thermal expansivity was also considered.

When the viscosity reduction is not incorporated, viscous resistance in the deepest mantle substantially controls the lithosphere motion in the case with the yield strength of 300 MPa. The large yield strength causes that the plate motion averaged in time is maintained to be less than 5 cm/yr, except in the cases with the viscosity of the lowermost mantle less than 10^{22} Pa s. Furthermore, the horizontal motion in the lowermost region is equivalent to half value of that of the surface plate. When the yield strength is set to 200 MPa, the viscosity increase in the lower mantle generates periodic slab folds by sharp bending. This substantially absorbs difference in the motion between the surface and the lowermost mantle. The slab folding generates a lump of the subducted lithosphere, which has large negative buoyancy. Toppling of the slab lump colliding the core-mantle boundary induces episodic acceleration of the slab descent motion. At this time, the plate motion exceeds 10 cm/yr. The slab is regarded as a stress guide between the surface and lowermost mantle in spite of the deformation. The slab interaction with the CMB region would therefore appear to the surface as significant fluctuation of the plate motion. Although the slab folds are generated when the depth-dependent thermal expansivity is introduced with the yield strength of 300 MPa, the decoupling between the surface and lowermost mantle motion is not enough to explain the stationary hotspot.

When viscosity reduction beneath the 660-km phase boundary is introduced, the viscous resistance of the deep mantle is not transmitted to the surface. The viscosity of the uppermost lower mantle controls the speed of the plate motion in the range of 5 to 10 cm/yr, which is consistent with the observation. On the contrary, the speed of the deep mantle flow is reduced to about 1/5 of the surface plate motion. Slab deformation induced by the viscosity reduction is therefore an important mechanism to weaken the

coupling between the plate and deep mantle and to regulate subducting plate motion.

キーワード：マントル対流、プレート運動、下部マントル、スラブ、レオロジー
Keywords: mantle convection, plate motion, lower mantle, subducted slab, rheology

Detection of Hadean crustal material in the deep Earth and Moon

*趙 大鵬[1]、磯崎 行雄[2]、丸山 茂徳[3]
*Dapeng Zhao[1], Yukio Isozaki[2], Shigenori Maruyama[3]

1. 東北大学大学院理学研究科附属地震・噴火予知研究観測センター、2. 東京大学大学院総合文化研究科、3. 東京工業大学地球生命研究所
1. Department of Geophysics, Tohoku University, 2. Department of General System Studies, The University of Tokyo, 3. Earth-Life Science Institute, Tokyo Institute of Technology

Because of the tectonic erosion associated with plate subductions, the Hadean crustal material may have been brought down to the deep interior of the Earth (Kawai et al., 2009, 2013; Isozaki et al., 2010; Dohm and Maruyama, 2015; Maruyama and Ebisuzaki, 2017; Maruyama et al., 2017). The primordial material may have physical properties different from those of the surrounding mantle rocks, hence it could be detected using seismic tomography.

Significant lateral variations of S-wave velocity (Vs) are revealed in the lunar mantle by tomographic imaging (Zhao et al., 2008, 2012). A correlation between the Vs tomography and the thorium abundance distribution is found. The area with a high thorium abundance exhibits a distinct low Vs zone which extends down to a depth of ~300 km below the Procellarum KREEP Terrane (PKT), which may reflect a thermal and compositional anomaly beneath the PKT. The distribution of deep moonquakes shows a correlation with the tomography in the deep lunar mantle, similar to earthquakes which are affected by structural heterogeneities in the terrestrial crust and upper mantle. The occurrence of deep moonquakes and seismic-velocity heterogeneities implies that the lunar interior may contain a certain amount of fluids and so still be thermally and dynamically active at present. Because there is no plate tectonics in the Moon, the Hadean crustal material may have been preserved near the lunar surface till today. However, due to the mantle overturn that happened at the early stage of the Moon, part of the Hadean crustal KREEP material may have sunk to the deep mantle, which may have become heat sources for the lunar mantle activities and so caused the deep moonquakes around them.

The processes happened in the Moon may have also taken place in the deep Earth. Due to the plate subductions, the Hadean crustal KREEP material may have sunk to the deep mantle of the Earth, which may have become heat sources for mantle plumes and super-plumes. Prominent low seismic-velocity (low-V) anomalies are clearly revealed in the deep mantle beneath the surface hotspot regions such as south-central Pacific, East Africa, Hawaii and Iceland (Zhao et al., 2013; Zhao, 2015). Some of the low-V anomalies could be caused by the Hadean crustal KREEP material.

References

Dohm, J.M., S. Maruyama (2015) Habitable trinity. *Geoscience Frontiers* 6, 95-101.

Isozaki, Y., K. Aoki, T. Nakama, S. Yanai (2010) New insight into a subduction-related orogen: A reappraisal of the geotectonic framework and evolution of the Japanese Islands. *Gondwana Res.* 18, 82-105.

Kawai, K., T. Tsuchiya, J. Tsuchiya, S. Maruyama (2009) Lost primordial continents. *Gondwana Res.* 16, 581-586.

Kawai, K., S. Yamamoto, T. Tsuchiya, S. Maruyama (2013) The second continent: Existence of granitic continental materials around the bottom of the mantle transition zone. *Geoscience Frontiers* 4, 1-6.

Maruyama, S., T. Ebisuzaki (2017) Origin of the Earth: a proposal of new model called ABEL. *Geoscience Frontiers*. http://dx.doi.org/10.1016/j.gsf.2016.10.005.

Maruyama, S., M. Santosh, S. Azuma (2017) Initiation of plate tectonics in the Hadean: Eclogitization triggered by the ABEL Bombardment. *Geoscience Frontiers*.
http://dx.doi.org/10.1016/j.gsf.2016.11.009.

Zhao, D. (2015) *Multiscale Seismic Tomography*. Springer, 304 pp.
Zhao, D., J. Lei, L. Liu (2008) Seismic tomography of the Moon. *Chinese Sci. Bull.* 53, 3897-3907.
Zhao, D., T. Arai, L. Liu, E. Ohtani (2012) Seismic tomography and geochemical evidence for lunar mantle heterogeneity: Comparing with Earth. *Global Planet. Change* 90, 29-36.
Zhao, D., Y. Yamamoto, T. Yanada (2013) Global mantle heterogeneity and its influence on teleseismic regional tomography. *Gondwana Res.* 23, 595-616.

キーワード：冥王代の地殻、月震、地震波トモグラフィー、KREEP、トリウム
Keywords: Hadean crust, moonquake, seismic tomography, KREEP, thorium

Grain growth kinetics in pyrolite composition: Implications for grain-size evolution of lower-mantle slab

*今村 公裕[1]、久保 友明[1]
*Masahiro Imamura[1], Tomoaki Kubo[1]

1. 九州大学
1. Kyushu University

Viscosity of lower-mantle slab largely depends on grain size in constituent minerals. It consists of bridgmanite (Brg), ferro-periclase (Fp), Ca-perovskite (Capv), and majoritic garnet (Mjgt) in the case of pyrolite composition. The grain-size evolution of lower-mantle slab is mainly controlled by grain growth process after the significant grain-size reduction due to the post-spinel transformation. Grain growth kinetics can be described by $d^n-d_0^n=kt$ (d: grain size, d_0: initial grain size,n: grain growth exponent, k: Arrhenius-type rate constant, t: time). In the multiphase system, Zener pinning is an important process and grain growth of the primary phase is controlled by Ostwald ripening of the secondary phase, which can be described by $d_I/d_{II}=\beta/f_{II}^z$ (d_I: grain size of primary phase, d_{II}: grain size of secondary phase, f_{II}: volume fraction of secondary phase, β and z: Zener parameters). In the present study, we conducted grain growth experiments in pyrolite composition under lower mantle conditions, and discuss the grain-size evolution of lower-mantle slab.

Annealing experiments in pyrolitic material were conducted at 25-27 GPa and 1600-1950˚C for 30-3000 min using a Kawai-type apparatus at Kyushu University. FE-SEM was used for microstructural observations and chemical analysis. Four phases of Brg (~70 vol%), Fp (~15 vol%), Mjgt (~13 vol%), and Capv (~2 vol%) were observed in recovered samples annealed at 25 GPa. To avoid the effects of the eutectoid texture on the kinetics, we took the grain growth data only from the sample exhibiting relatively homogeneous polygonal texture. Both secondary phases of Fp and Mjgt are homogeneously distributed in the Brg-dominant sample after the polygonal texture was achieved. The grain size ratio of d_{Brg}/d_{Fp} and d_{Brg}/d_{Mjgt} are almost constant during the grain growth and estimated to be ~1.7 and ~1.2, respectively. These microstructural observations imply that the Brg grain growth is pinned by the secondary phases, and the rate is controlled by Ostwald ripening kinetics. We obtained n values of 6.2, 3.3, and 3.1 for Brg, Fp, and Mjgt, respectively. The averaged n value of ~4.2 is consistent with the multiphase grain growth model when the secondary phase grows by Ostwald ripening process (n=4, grain-boundary diffusion controlled). When assuming the n-value of 4, the activation enthalpies for Brg, Fp, and Mjgt are estimated to be ~410, ~240, and ~500 kJ/mol, respectively, implying that the rate-controlling species are different between Ostwald ripening processes of Fp and Mjgt, and the Brg grain growth is controlled by both processes. If we treat Fp and Mjgt as a secondary phase ($d_{II=Fp+Mjgt}$) ignoring Capv, the activation enthalpies are almost the same between the primary and secondary phases. The grain size ratio of $d_{I=Brg}/d_{II=Fp+Mjgt}$ is ~1.5 with the $f_{II=Fp+Mjgt}$ of 0.3, which is almost consistent with the previous systematic study in the olivine-enstatite system (Tasaka and Hiraga, 2013). On the other hand, three phases without Mjgt were present at higher pressure of 27 GPa, in which the grain size was slightly larger probably due to the smaller proportion of the secondary phases (~77 vol% of Brg).

On the basis of the results obtained above, we estimated grain-size evolution of lower-mantle slab assuming that Zener parameters are the same as the previous study (Tasaka and Hiraga, 2013). The grain size of Brg in a pyrolitic composition with ($f_{II=Fp+Mjgt}$=0.3) and without ($f_{II=Fp}$=0.2) bearing Mjgt is estimated to be ~5-650 μm and ~50-900 μm, respectively, at 800-1600˚C in 10^8 years. When considering an olivine-like ($f_{II=Fp}$=0.3) and a perovskitic ($f_{II=Fp}$=0.1) compositions, the Brg grain size decreases to ~40-720 μm and increases to ~80-1270 μm, respectively. Thus, the grain size in lower-mantle slab is likely kept

smaller than 1 mm, suggesting that grain-size sensitive creep is dominant. Viscosity variations in lower-mantle slab will be discussed considering a dynamic grain-growth effect.

A revisit on initial temperature at the core-mantle boundary in a coupled core-mantle evolution model

*中川 貴司[1]
*Takashi Nakagawa[1]

1. 海洋研究開発機構数理科学・先端技術研究分野
1. MAT, JAMSTEC

An initial temperature at the core-mantle boundary (CMB) is an important constraint for thermal evolution of Earth’s mantle and core because this temperature strongly affects the size and onset timing of growing inner core, primordial heat in early Earth’s core and thermal and chemical state in the deep mantle. In a previous study, we found ~6000 K as the initial CMB temperature in a coupled core-mantle evolution model to match constraints of thermal evolution of Earth’s core [Nakagawa and Tackley, 2010]. However, in recent suggestions from high P-T physics and theoretical model of thermal evolution of Earth’s core, the initial CMB temperature seems to be less than ~5000 K [Andrault et al., 2016; Nakagawa, in revisoin]. Since our core evolution model is based on a simplified analytical formulation [Buffett et al., 1992; Buffett et al., 1996] and more complicated formulation that can fit the density structure derived from seismological analysis and applicable for high thermal conductivity of iron alloy is proposed [Labrosse, 2015], we reassess the initial CMB temperature that can find the best-fit core evolution scenario. Because of thermostat effects on thermal evolution [e.g. Nakagawa and Tackley, 2010; Nakagawa and Tackley, 2012], the initial CMB temperature may not be sensitive to the scenario of thermal evolution of Earth’s core and mantle but the heat flow across the CMB found in this study (9 to 10 TW) is slightly lower than the lower-bound value (11 TW). On the magnetic evolution, the low thermal conductivity is still more preferable than high thermal conductivity due to existence of adiabatic shell with high thermal conductivity that suppress a convective region of Earth’s core. In the presentation, we will attempt to an implication for detectability of geoneutrino based on thermal and chemical evolution modeling of Earth’s mantle and core.

キーワード：コアーマントル境界温度、熱進化、地球金属核
Keywords: core-mantle boundary temperature, thermal evolution, Earth's metallic core

